

Solving a non-linear model of HIV infection for CD4⁺T cells by combining Laplace transformation and Homotopy analysis method

Samad Noeiaghdam^{1, *}

Emran Khoshrouye Ghiasi^{2, †}

¹ Department of Mathematics, Central Tehran Branch, Islamic Azad University, Tehran, Iran.

² Young Researchers and Elite Club, Mashhad Branch, Islamic Azad University, Mashhad, Iran.

Abstract

The aim of this paper is to find the approximate solution of HIV infection model of CD4⁺T cells. For this reason, the homotopy analysis transform method (HATM) is applied. The presented method is combination of traditional homotopy analysis method (HAM) and the Laplace transformation. The convergence of presented method is discussed by preparing a theorem which shows the capabilities of method. The numerical results are shown for different values of iterations. Also, the regions of convergence are demonstrated by plotting several h -curves. Furthermore in order to show the efficiency and accuracy of method, the residual error for different iterations are presented.

keywords: Homotopy analysis method Laplace transformation System of non-linear differential equations HIV infection model of CD4⁺T cells.

MSC codes (2000): 92B05, 65L99, 44A10.

1 Introduction

In last decades, many natural phenomena have been described by various nonlinear mathematical models such as the human immunodeficiency virus (HIV) [5, 45, 53, 55, 57, 58], mathematical model of smoking habit [18, 52, 54], model of malaria transmission [56], model of computer viruses [15, 19, 41, 47] and many mathematical models that have direct role in our life. Perelson in 1989 presented a model for infection of human immune system by HIV which was based on the three variables [49]. Then Perelson et al. modified and generalized this model to new model with four variables by a system of non-linear ordinary differential equations [50]. In recent years, several applicable models have been presented based on the Perelson's models [6]. Also, many numerical and semi-analytical methods have been applied to solve the vivo dynamics of T -cell

*Corresponding author, E-mail addresses: s.noeiaghdam.sci@iauctb.ac.ir; samadnoeiaghdam@gmail.com

†E-mail address: khoshrou@yahoo.com

and HIV interaction. The aim of this paper is to solve the Culshaw and Ruan's model [6] for HIV infection of $CD4^+$ T-cells as

$$\begin{aligned}\frac{d\mathcal{T}(c)}{dc} &= s - \omega_{\mathcal{T}}\mathcal{T}(c) + g\mathcal{T}(c) \left(1 - \frac{\mathcal{I}(c) + \mathcal{T}(c)}{\mathcal{T}_{\max}}\right) - \alpha\mathcal{V}(c)\mathcal{T}(c), \\ \frac{d\mathcal{I}(c)}{dc} &= \beta\mathcal{V}(c)\mathcal{T}(c) - \omega_I\mathcal{I}(c), \\ \frac{d\mathcal{V}(c)}{dc} &= n\omega_b\mathcal{I}(c) - \alpha\mathcal{V}(c)\mathcal{T}(c) - \omega_{\mathcal{V}}\mathcal{V}(c),\end{aligned}\tag{1}$$

with the initial conditions

$$\mathcal{T}(0) = \mathcal{T}_0(c) = \mathcal{T}_0, \mathcal{I}(0) = \mathcal{I}_0(c) = \mathcal{I}_0, \mathcal{V}(0) = \mathcal{V}_0(c) = \mathcal{V}_0.\tag{2}$$

Functions $\mathcal{T}(c)$, $\mathcal{I}(c)$, and $\mathcal{V}(c)$ show the concentration of susceptible $CD4^+$ T cells, $CD4^+$ T cells infected by the HIV viruses and free HIV virus particles in the blood, respectively. List of parameters are presented in Table 1.

Table 1: List of parameters and functions.

Parameters & Functions	Meaning	Values
\mathcal{T}	Uninfected $CD4^+$ T-cell concentration	$\mathcal{T}_0 = 1000$
\mathcal{I}	Infected $CD4^+$ T-cell concentration	$\mathcal{I}_0 = 0$
\mathcal{V}	Concentration of HIV RNA	$\mathcal{V}_0 = 0.001$
$\omega_{\mathcal{T}}$	Natural death rate of $CD4^+$ T-cell concentration	0.02
ω_I	Blanket death rate of infected $CD4^+$ T-cells	0.26
ω_b	Lytic death rate for infected cells	0.24
$\omega_{\mathcal{V}}$	Death rate of free virus	2.4
α	Rate $CD4^+$ T-cells become infected with virus	2.4×10^{-5}
β	Rate infected cells become active	2×10^{-5}
g	Growth rate of $CD4^+$ T-cell concentration	0.03
n	Number of virion produced by infected $CD4^+$ T-cells	500
\mathcal{T}_{\max}	Maximal concentration of $CD4^+$ T-cells	1500
s	Source term for uninfected $CD4^+$ T-cells	10

Solving problem (1) has been studied by many authors. Several mathematical methods such as the Adomian decomposition method (ADM) [5, 7, 45], HAM [17], variational iteration method (VIM) [40], collocation method (CM) [8, 48, 51, 55, 57], differential transform method (DTM) [16, 53, 59] and other [58] were applied to solve the system of Eqs. (1).

The HAM [1, 2, 3, 9, 10, 11, 12, 14, 42] is an important and useful method to solve many problems [22, 23, 24, 25, 26, 27, 28]. The solution of this method contains the optimal convergence control parameter to find the region of convergence. Also this method depends on the auxiliary function and linear operator to find the solution. Choosing the proper function and operator can be leaded to the solution quickly. These are the important capabilities of HAM that the other traditional methods do not have these advantages.

In this paper, HAM is combined with the Laplace transformation [4, 21, 29, 30, 46] to construct a new and robust method which is called the homotopy analysis transform method (HATM) [13, 31, 32, 44]. This method applied to solve many problems arising in engineering and many sciences [20, 33, 34]. In this study, by using the HATM we try to solve the non-linear system of Eqs. (1) and the numerical solutions for $N = 5, 10, 15$ are obtained. The convergence theorem warranties the homotopy analysis transform method theoretically. Several h -curves are plotted to show the regions of convergence. Also, in order to show the efficiency and accuracy of HATM, the residual error functions are applied for different values based on the regions of convergence.

2 Homotopy analysis transform method

In order to apply the HATM for solving system of Eqs. (1), the Laplace transformation \mathcal{L} is used as follows

$$\begin{aligned}
\mathcal{L}[\mathcal{T}(c)] &= \frac{\mathcal{T}(0)}{z} + \frac{\mathcal{L}[s]}{z} + \frac{(g - \omega_{\mathcal{T}})}{z} \mathcal{L}[\mathcal{T}(c)] - \frac{g}{z\mathcal{T}_{\max}} \mathcal{L}[\mathcal{T}^2(c)] \\
&\quad - \frac{g}{z\mathcal{T}_{\max}} \mathcal{L}[\mathcal{T}(c)\mathcal{I}(c)] - \frac{\alpha}{z} \mathcal{L}[\mathcal{V}(c)\mathcal{T}(c)], \\
\mathcal{L}[\mathcal{I}(c)] &= \frac{\mathcal{I}(0)}{z} + \frac{\beta}{z} \mathcal{L}[\mathcal{V}(c)\mathcal{T}(c)] - \frac{\omega_{\mathcal{I}}}{z} \mathcal{L}[\mathcal{I}(c)], \\
\mathcal{L}[\mathcal{V}(c)] &= \frac{\mathcal{V}(0)}{z} + \frac{n\omega_b}{z} \mathcal{L}[\mathcal{I}(c)] - \frac{\alpha}{z} \mathcal{L}[\mathcal{V}(c)\mathcal{T}(c)] - \frac{\omega_{\mathcal{V}}}{z} \mathcal{L}[\mathcal{V}(c)].
\end{aligned} \tag{3}$$

According to [35, 36, 37, 38, 39] we define the following non-linear operators N_1, N_2 and N_3 as

$$\begin{aligned}
& N_1 \left[\mathcal{T}(c; \eta), \mathcal{I}(c; \eta), \mathcal{V}(c; \eta) \right] \\
&= \mathcal{L} \left[\mathcal{T}(c; \eta) \right] - \frac{\mathcal{T}(0)}{z} - \frac{\mathcal{L} \left[s \right]}{z} - \frac{(g - \omega_{\mathcal{T}})}{z} \mathcal{L} \left[\mathcal{T}(c; \eta) \right] + \frac{g}{z \mathcal{T}_{\max}} \mathcal{L} \left[\mathcal{T}^2(c; \eta) \right] \\
&+ \frac{g}{z \mathcal{T}_{\max}} \mathcal{L} \left[\mathcal{T}(c; \eta) \mathcal{I}(c; \eta) \right] + \frac{\alpha}{z} \mathcal{L} \left[\mathcal{V}(c; \eta) \mathcal{T}(c; \eta) \right], \\
& N_2 \left[\mathcal{T}(c; \eta), \mathcal{I}(c; \eta), \mathcal{V}(c; \eta) \right] \\
&= \mathcal{L} \left[\mathcal{I}(c; \eta) \right] - \frac{\mathcal{I}(0)}{z} - \frac{\beta}{z} \mathcal{L} \left[\mathcal{V}(c; \eta) \mathcal{T}(c; \eta) \right] + \frac{\omega_{\mathcal{I}}}{z} \mathcal{L} \left[\mathcal{I}(c; \eta) \right], \\
& N_3 \left[\mathcal{T}(c; \eta), \mathcal{I}(c; \eta), \mathcal{V}(c; \eta) \right] \\
&= \mathcal{L} \left[\mathcal{V}(c; \eta) \right] - \frac{\mathcal{V}(0)}{z} - \frac{n\omega_b}{z} \mathcal{L} \left[\mathcal{I}(c; \eta) \right] + \frac{\alpha}{z} \mathcal{L} \left[\mathcal{V}(c; \eta) \mathcal{T}(c; \eta) \right] + \frac{\omega_{\mathcal{V}}}{z} \mathcal{L} \left[\mathcal{V}(c; \eta) \right],
\end{aligned} \tag{4}$$

where $\eta \in [0, 1]$ is an imbedding parameter. Now the following homotopy maps can be constructed as

$$\begin{aligned}
& \mathcal{H}_1 \left(\tilde{\mathcal{T}}(c; \eta), \tilde{\mathcal{I}}(c; \eta), \tilde{\mathcal{V}}(c; \eta) \right) \\
&= (1 - \eta) L_1 \left[\tilde{\mathcal{T}}(c; \eta) - \mathcal{T}_0(c) \right] - \eta \hbar H_1(c) N_1 \left[\tilde{\mathcal{T}}(c; \eta), \tilde{\mathcal{I}}(c; \eta), \tilde{\mathcal{V}}(c; \eta) \right], \\
& \mathcal{H}_2 \left(\tilde{\mathcal{T}}(c; \eta), \tilde{\mathcal{I}}(c; \eta), \tilde{\mathcal{V}}(c; \eta) \right) \\
&= (1 - \eta) L_2 \left[\tilde{\mathcal{I}}(c; \eta) - \mathcal{I}_0(c) \right] - \eta \hbar H_2(c) N_2 \left[\tilde{\mathcal{T}}(c; \eta), \tilde{\mathcal{I}}(c; \eta), \tilde{\mathcal{V}}(c; \eta) \right], \\
& \mathcal{H}_3 \left(\tilde{\mathcal{T}}(c; \eta), \tilde{\mathcal{I}}(c; \eta), \tilde{\mathcal{V}}(c; \eta) \right) \\
&= (1 - \eta) L_3 \left[\tilde{\mathcal{V}}(c; \eta) - \mathcal{V}_0(c) \right] - \eta \hbar H_3(c) N_3 \left[\tilde{\mathcal{T}}(c; \eta), \tilde{\mathcal{I}}(c; \eta), \tilde{\mathcal{V}}(c; \eta) \right],
\end{aligned} \tag{5}$$

where \hbar is a nonzero auxiliary parameter, H_1, H_2, H_3 are auxiliary functions and N_1, N_2, N_3 are non-linear operators. When

$$\begin{aligned}\mathcal{H}_1\left(\tilde{\mathcal{T}}(c; \eta), \tilde{\mathcal{I}}(c; \eta), \tilde{\mathcal{V}}(c; \eta)\right) &= \mathcal{H}_2\left(\tilde{\mathcal{T}}(c; \eta), \tilde{\mathcal{I}}(c; \eta), \tilde{\mathcal{V}}(c; \eta)\right) \\ &= \mathcal{H}_3\left(\tilde{\mathcal{T}}(c; \eta), \tilde{\mathcal{I}}(c; \eta), \tilde{\mathcal{V}}(c; \eta)\right) = 0,\end{aligned}$$

the zero order deformation equations are obtained

$$\begin{aligned}(1 - \eta)L_1\left[\tilde{\mathcal{T}}(c; \eta) - \mathcal{T}_0(c)\right] - \eta\hbar H_1(c)N_1\left[\tilde{\mathcal{T}}(c; \eta), \tilde{\mathcal{I}}(c; \eta), \tilde{\mathcal{V}}(c; \eta)\right] &= 0, \\ (1 - \eta)L_2\left[\tilde{\mathcal{I}}(c; \eta) - \mathcal{I}_0(c)\right] - \eta\hbar H_2(c)N_2\left[\tilde{\mathcal{T}}(c; \eta), \tilde{\mathcal{I}}(c; \eta), \tilde{\mathcal{V}}(c; \eta)\right] &= 0, \\ (1 - \eta)L_3\left[\tilde{\mathcal{V}}(c; \eta) - \mathcal{V}_0(c)\right] - \eta\hbar H_3(c)N_3\left[\tilde{\mathcal{T}}(c; \eta), \tilde{\mathcal{I}}(c; \eta), \tilde{\mathcal{V}}(c; \eta)\right] &= 0.\end{aligned}\tag{6}$$

Also, for $\eta = 0$ and $\eta = 1$ the homotopy equations lead to

$$\begin{aligned}\tilde{\mathcal{T}}(c; 0) &= \mathcal{T}_0(c), & \tilde{\mathcal{T}}(c; 1) &= \mathcal{T}(c), \\ \tilde{\mathcal{I}}(c; 0) &= \mathcal{I}_0(c), & \tilde{\mathcal{I}}(c; 1) &= \mathcal{I}(c), \\ \tilde{\mathcal{V}}(c; 0) &= \mathcal{V}_0(c), & \tilde{\mathcal{V}}(c; 1) &= \mathcal{V}(c).\end{aligned}$$

Therefore, when η changes from 0 to 1 the initial functions $\mathcal{T}_0(c), \mathcal{I}_0(c), \mathcal{V}_0(c)$ lead to the exact solutions $\mathcal{T}(c), \mathcal{I}(c), \mathcal{V}(c)$. By applying the Taylor series for $\tilde{\mathcal{T}}(c; \eta), \tilde{\mathcal{I}}(c; \eta), \tilde{\mathcal{V}}(c; \eta)$ with respect to η we get

$$\begin{aligned}\tilde{\mathcal{T}}(c; \eta) &= \mathcal{T}_0(c) + \sum_{d=1}^{\infty} \mathcal{T}_d(c)\eta^d, \\ \tilde{\mathcal{I}}(c; \eta) &= \mathcal{I}_0(c) + \sum_{d=1}^{\infty} \mathcal{I}_d(c)\eta^d, \\ \tilde{\mathcal{V}}(c; \eta) &= \mathcal{V}_0(c) + \sum_{d=1}^{\infty} \mathcal{V}_d(c)\eta^d,\end{aligned}\tag{7}$$

where

$$\mathcal{T}_d = \frac{1}{d!} \frac{\partial^d \tilde{\mathcal{T}}(c; \eta)}{\partial \eta^d} \Big|_{\eta=0}, \quad \mathcal{I}_d = \frac{1}{d!} \frac{\partial^d \tilde{\mathcal{I}}(c; \eta)}{\partial \eta^d} \Big|_{\eta=0}, \quad \mathcal{V}_d = \frac{1}{d!} \frac{\partial^d \tilde{\mathcal{V}}(c; \eta)}{\partial \eta^d} \Big|_{\eta=0}.$$

For proper value, operator and functions of $\hbar, L, H_1(c), H_2(c), H_3(c)$ relations (7) are convergent at $\eta = 1$. For more analysis, the following vectors are defined as

$$\tilde{\mathcal{T}}_N(c) = \left\{ \mathcal{T}_0(c), \mathcal{T}_1(c), \dots, \mathcal{T}_N(c) \right\},$$

$$\tilde{\mathcal{I}}_N(c) = \left\{ \mathcal{I}_0(c), \mathcal{I}_1(c), \dots, \mathcal{I}_N(c) \right\},$$

$$\tilde{\mathcal{V}}_N(c) = \left\{ \mathcal{V}_0(c), \mathcal{V}_1(c), \dots, \mathcal{V}_N(c) \right\}.$$

Differentiating the Eqs. (6) d -times with respect to η , dividing by $d!$ and putting $\eta = 0$ the d -th order deformation equations for vectors $\vec{\mathcal{T}}, \vec{\mathcal{I}}, \vec{\mathcal{V}}$ can be obtained

$$\begin{aligned} L_1 [\mathcal{T}_d(c) - \chi_d \mathcal{T}_{d-1}(c)] &= \hbar H_1(c) \mathfrak{R}_d^1 \left(\vec{\mathcal{T}}_{d-1}, \vec{\mathcal{I}}_{d-1}, \vec{\mathcal{V}}_{d-1} \right), \\ L_2 [\mathcal{I}_d(c) - \chi_d \mathcal{I}_{d-1}(c)] &= \hbar H_2(c) \mathfrak{R}_d^2 \left(\vec{\mathcal{T}}_{d-1}, \vec{\mathcal{I}}_{d-1}, \vec{\mathcal{V}}_{d-1} \right), \\ L_3 [\mathcal{V}_d(c) - \chi_d \mathcal{V}_{d-1}(c)] &= \hbar H_3(c) \mathfrak{R}_d^3 \left(\vec{\mathcal{T}}_{d-1}, \vec{\mathcal{I}}_{d-1}, \vec{\mathcal{V}}_{d-1} \right), \end{aligned} \tag{8}$$

where

$$\mathcal{T}_d(0) = 0, \quad \mathcal{I}_d(0) = 0, \quad \mathcal{V}_d(0) = 0,$$

and

$$\begin{aligned}
\Re_d^1(c) &= \mathcal{L} \left[\mathcal{T}_{d-1}(c) \right] - \frac{\mathcal{T}_{d-1}(0)}{z} - (1 - \chi_d) \frac{\mathcal{L} \left[s \right]}{z} - \frac{(g - \omega \mathcal{T})}{z} \mathcal{L} \left[\mathcal{T}_{d-1}(c) \right] \\
&\quad + \frac{g}{z \mathcal{T}_{\max}} \mathcal{L} \left[\sum_{p=0}^{d-1} \mathcal{T}_p(c) \mathcal{T}_{d-1-p}(c) \right] + \frac{g}{z \mathcal{T}_{\max}} \mathcal{L} \left[\sum_{p=0}^{d-1} \mathcal{T}_p(c) \mathcal{I}_{d-1-p}(c) \right] \\
&\quad + \frac{\alpha}{z} \mathcal{L} \left[\sum_{p=0}^{d-1} \mathcal{V}_p(c) \mathcal{T}_{d-1-p}(c) \right], \\
\Re_d^2(c) &= \mathcal{L} \left[\mathcal{I}_{d-1}(c) \right] - \frac{\mathcal{I}_{d-1}(0)}{z} - \frac{\beta}{z} \mathcal{L} \left[\sum_{p=0}^{d-1} \mathcal{V}_p(c) \mathcal{T}_{d-1-p}(c) \right] \\
&\quad + \frac{\omega \mathcal{I}}{z} \mathcal{L} \left[\mathcal{I}_{d-1}(c) \right], \\
\Re_d^3(c) &= \mathcal{L} \left[\mathcal{V}_{d-1}(c) \right] - \frac{\mathcal{V}_{d-1}(0)}{z} - \frac{n \omega_b}{z} \mathcal{L} \left[\mathcal{I}_{d-1}(c) \right] \\
&\quad + \frac{\alpha}{z} \mathcal{L} \left[\sum_{p=0}^{d-1} \mathcal{V}_p(c) \mathcal{T}_{d-1-p}(c) \right] + \frac{\omega \mathcal{V}}{z} \mathcal{L} \left[\mathcal{V}_{d-1}(c) \right],
\end{aligned} \tag{9}$$

and

$$\chi_d = \begin{cases} 0, & d \leq 1 \\ 1, & d > 1. \end{cases}$$

Using $H_1(c) = H_2(c) = H_3(c) = 1$ and applying the inverse operator $L^{-1} = \mathcal{L}^{-1}$ the solutions of d -th order deformation equations (8) are obtained as

$$\begin{aligned}
&\mathcal{T}_d(c) - \chi_d \mathcal{T}_{d-1}(c) \\
&= \hbar \left\{ \mathcal{T}_{d-1}(c) - (1 - \chi_d) \mathcal{L}^{-1} \left[\frac{\mathcal{L} \left[s \right]}{z} \right] - \mathcal{L}^{-1} \left[\frac{(g - \omega \mathcal{T})}{z} \mathcal{L} \left[\mathcal{T}_{d-1}(c) \right] \right] \right. \\
&\quad + \mathcal{L}^{-1} \left[\frac{g}{z \mathcal{T}_{\max}} \mathcal{L} \left[\sum_{p=0}^{d-1} \mathcal{T}_p(c) \mathcal{T}_{d-1-p}(c) \right] \right] \\
&\quad \left. + \mathcal{L}^{-1} \left[\frac{g}{z \mathcal{T}_{\max}} \mathcal{L} \left[\sum_{p=0}^{d-1} \mathcal{T}_p(c) \mathcal{I}_{d-1-p}(c) \right] \right] + \mathcal{L}^{-1} \left[\frac{\alpha}{z} \mathcal{L} \left[\sum_{p=0}^{d-1} \mathcal{V}_p(c) \mathcal{T}_{d-1-p}(c) \right] \right] \right\},
\end{aligned}$$

$$\begin{aligned}
& \mathcal{I}_d(c) - \chi_d \mathcal{I}_{d-1}(c) \\
&= \hbar \left\{ \mathcal{I}_{d-1}(c) - \mathcal{L}^{-1} \left[\frac{\beta}{z} \mathcal{L} \left[\sum_{p=0}^{d-1} \mathcal{V}_p(c) \mathcal{T}_{d-1-p}(c) \right] \right] + \mathcal{L}^{-1} \left[\frac{\omega \mathcal{I}}{z} \mathcal{L} \left[\mathcal{I}_{d-1}(c) \right] \right] \right\}, \\
& \mathcal{V}_d(c) - \chi_d \mathcal{V}_{d-1}(c) \\
&= \hbar \left\{ \mathcal{V}_{d-1}(c) - \mathcal{L}^{-1} \left[\frac{n\omega_b}{z} \mathcal{L} \left[\mathcal{I}_{d-1}(c) \right] \right] + \mathcal{L}^{-1} \left[\frac{\alpha}{z} \mathcal{L} \left[\sum_{p=0}^{d-1} \mathcal{V}_p(c) \mathcal{T}_{d-1-p}(c) \right] \right] \right. \\
& \quad \left. + \mathcal{L}^{-1} \left[\frac{\omega \mathcal{V}}{z} \mathcal{L} \left[\mathcal{V}_{d-1}(c) \right] \right] \right\}.
\end{aligned} \tag{10}$$

Finally, the N -th order of approximate solutions can be obtained by

$$\mathcal{T}_N(c) = \sum_{p=0}^N \mathcal{T}_p(c), \quad \mathcal{I}_N(c) = \sum_{p=0}^N \mathcal{I}_p(c), \quad \mathcal{V}_N(c) = \sum_{p=0}^N \mathcal{V}_p(c). \tag{11}$$

3 Convergence theorem

In this section, by presenting a theorem, convergence of HATM to solve the non-linear system of equations (1) is illustrated.

Theorem 1. *If series solutions*

$$\begin{aligned}
\mathcal{T}(c) &= \mathcal{T}_0(c) + \sum_{d=1}^{\infty} \mathcal{T}_d(c), \\
\mathcal{I}(c) &= \mathcal{I}_0(c) + \sum_{d=1}^{\infty} \mathcal{I}_d(c), \\
\mathcal{V}(c) &= \mathcal{V}_0(c) + \sum_{d=1}^{\infty} \mathcal{V}_d(c),
\end{aligned} \tag{12}$$

are convergent where $\mathcal{T}_d(c), \mathcal{I}_d(c), \mathcal{V}_d(c)$ are formed by Eqs. (8), then they must be the exact solution of system (1).

Proof: Assume that the series solutions (12) are convergent. Therefore we get

$$S_1(c) = \sum_{d=0}^{\infty} \mathcal{T}_d(c), \quad S_2(c) = \sum_{d=0}^{\infty} \mathcal{I}_d(c), \quad S_3(c) = \sum_{d=0}^{\infty} \mathcal{V}_d(c), \tag{13}$$

where we have

$$\lim_{d \rightarrow \infty} \mathcal{T}_d(c) = 0, \quad \lim_{d \rightarrow \infty} \mathcal{I}_d(c) = 0, \quad \lim_{d \rightarrow \infty} \mathcal{V}_d(c) = 0. \tag{14}$$

By mentioned details of Section 2 we can write

$$\begin{aligned}
\sum_{d=1}^N \left[\mathcal{T}_d(c) - \chi_d \mathcal{T}_{d-1}(c) \right] &= \mathcal{T}_N(c), \\
\sum_{d=1}^N \left[\mathcal{I}_d(c) - \chi_d \mathcal{I}_{d-1}(c) \right] &= \mathcal{I}_N(c), \\
\sum_{d=1}^N \left[\mathcal{V}_d(c) - \chi_d \mathcal{V}_{d-1}(c) \right] &= \mathcal{V}_N(c),
\end{aligned} \tag{15}$$

which by using Eqs. (14) and (15) the following relations can be obtained

$$\begin{aligned}
\sum_{d=1}^N \left[\mathcal{T}_d(c) - \chi_d \mathcal{T}_{d-1}(c) \right] &= \lim_{N \rightarrow \infty} \mathcal{T}_N(c) = 0, \\
\sum_{d=1}^N \left[\mathcal{I}_d(c) - \chi_d \mathcal{I}_{d-1}(c) \right] &= \lim_{N \rightarrow \infty} \mathcal{I}_N(c) = 0, \\
\sum_{d=1}^N \left[\mathcal{V}_d(c) - \chi_d \mathcal{V}_{d-1}(c) \right] &= \lim_{N \rightarrow \infty} \mathcal{V}_N(c) = 0.
\end{aligned} \tag{16}$$

Since the operator L is a linear operator thus

$$\begin{aligned}
\sum_{d=1}^{\infty} L \left[\mathcal{T}_d(c) - \chi_d \mathcal{T}_{d-1}(c) \right] &= L \left[\sum_{d=1}^{\infty} \mathcal{T}_d(c) - \chi_d \mathcal{T}_{d-1}(c) \right] = 0, \\
\sum_{d=1}^{\infty} L \left[\mathcal{I}_d(c) - \chi_d \mathcal{I}_{d-1}(c) \right] &= L \left[\sum_{d=1}^{\infty} \mathcal{I}_d(c) - \chi_d \mathcal{I}_{d-1}(c) \right] = 0, \\
\sum_{d=1}^{\infty} L \left[\mathcal{V}_d(c) - \chi_d \mathcal{V}_{d-1}(c) \right] &= L \left[\sum_{d=1}^{\infty} \mathcal{V}_d(c) - \chi_d \mathcal{V}_{d-1}(c) \right] = 0,
\end{aligned} \tag{17}$$

and we can obtain

$$\begin{aligned}
\sum_{d=1}^{\infty} L_1 \left[\mathcal{T}_d(c) - \chi_d \mathcal{T}_{d-1}(c) \right] &= \hbar H_1(c) \sum_{d=1}^{\infty} \mathfrak{R}_d^1(\vec{\mathcal{T}}_{d-1}, \vec{\mathcal{I}}_{d-1}, \vec{\mathcal{V}}_{d-1}) = 0, \\
\sum_{d=1}^{\infty} L_2 \left[\mathcal{I}_d(c) - \chi_d \mathcal{I}_{d-1}(c) \right] &= \hbar H_2(c) \sum_{d=1}^{\infty} \mathfrak{R}_d^2(\vec{\mathcal{T}}_{d-1}, \vec{\mathcal{I}}_{d-1}, \vec{\mathcal{V}}_{d-1}) = 0, \\
\sum_{d=1}^{\infty} L_3 \left[\mathcal{V}_d(c) - \chi_d \mathcal{V}_{d-1}(c) \right] &= \hbar H_3(c) \sum_{d=1}^{\infty} \mathfrak{R}_d^3(\vec{\mathcal{T}}_{d-1}, \vec{\mathcal{I}}_{d-1}, \vec{\mathcal{V}}_{d-1}) = 0.
\end{aligned} \tag{18}$$

Since in Eqs. (18), $\hbar \neq 0, H_1(c) \neq 0, H_2(c) \neq 0, H_3(c) \neq 0$ we get

$$\begin{aligned}
\sum_{d=1}^{\infty} \mathfrak{R}_d^1(\vec{\mathcal{T}}_{d-1}, \vec{\mathcal{I}}_{d-1}, \vec{\mathcal{V}}_{d-1}) &= 0, \\
\sum_{d=1}^{\infty} \mathfrak{R}_d^2(\vec{\mathcal{T}}_{d-1}, \vec{\mathcal{I}}_{d-1}, \vec{\mathcal{V}}_{d-1}) &= 0, \\
\sum_{d=1}^{\infty} \mathfrak{R}_d^3(\vec{\mathcal{T}}_{d-1}, \vec{\mathcal{I}}_{d-1}, \vec{\mathcal{V}}_{d-1}) &= 0.
\end{aligned} \tag{19}$$

By putting $\mathfrak{R}_d^1(\mathcal{T}_{d-1}(c))$, $\mathfrak{R}_d^2(\mathcal{I}_{d-1}(c))$ and $\mathfrak{R}_d^3(\mathcal{V}_{d-1}(c))$ into Eqs. (19) we get

$$\begin{aligned}
& \sum_{d=1}^{\infty} \mathfrak{R}_d^1(\mathcal{T}_{d-1}(c)) \\
&= \sum_{d=1}^{\infty} \left[\mathcal{T}'_{d-1}(c) - (1 - \chi_d)s - (g - \omega_{\mathcal{T}})\mathcal{T}_{d-1}(c) + \frac{g}{\mathcal{T}_{\max}} \sum_{p=0}^{d-1} \mathcal{T}_p(c)\mathcal{T}_{d-1-p}(c) \right. \\
&\quad \left. + \frac{g}{\mathcal{T}_{\max}} \sum_{p=0}^{d-1} \mathcal{T}_p(c)\mathcal{I}_{d-1-p}(c) + \alpha \sum_{p=0}^{d-1} \mathcal{V}_p(c)\mathcal{T}_{d-1-p}(c) \right] \\
&= \sum_{d=0}^{\infty} \mathcal{T}'_d(c) - s - (g - \omega_{\mathcal{T}}) \sum_{d=0}^{\infty} \mathcal{T}_d(c) + \frac{g}{\mathcal{T}_{\max}} \sum_{d=1}^{\infty} \sum_{p=0}^{d-1} \mathcal{T}_p(c)\mathcal{T}_{d-1-p}(c) \\
&\quad + \frac{g}{\mathcal{T}_{\max}} \sum_{d=1}^{\infty} \sum_{p=0}^{d-1} \mathcal{T}_p(c)\mathcal{I}_{d-1-p}(c) + \alpha \sum_{d=1}^{\infty} \sum_{p=0}^{d-1} \mathcal{V}_p(c)\mathcal{T}_{d-1-p}(c) \\
&= \sum_{d=0}^{\infty} \mathcal{T}'_d(c) - s - (g - \omega_{\mathcal{T}}) \sum_{d=0}^{\infty} \mathcal{T}_d(c) + \frac{g}{\mathcal{T}_{\max}} \sum_{p=0}^{\infty} \sum_{d=p+1}^{\infty} \mathcal{T}_p(c)\mathcal{T}_{d-1-p}(c) \\
&\quad + \frac{g}{\mathcal{T}_{\max}} \sum_{p=0}^{\infty} \sum_{d=p+1}^{\infty} \mathcal{T}_p(c)\mathcal{I}_{d-1-p}(c) + \alpha \sum_{p=0}^{\infty} \sum_{d=p+1}^{\infty} \mathcal{V}_p(c)\mathcal{T}_{d-1-p}(c) \\
&= \sum_{d=0}^{\infty} \mathcal{T}'_d(c) - s - (g - \omega_{\mathcal{T}}) \sum_{d=0}^{\infty} \mathcal{T}_d(c) + \frac{g}{\mathcal{T}_{\max}} \sum_{p=0}^{\infty} \mathcal{T}_p(c) \sum_{d=0}^{\infty} \mathcal{T}_d(c) \\
&\quad + \frac{g}{\mathcal{T}_{\max}} \sum_{p=0}^{\infty} \mathcal{T}_p(c) \sum_{d=0}^{\infty} \mathcal{I}_d(c) + \alpha \sum_{p=0}^{\infty} \mathcal{V}_p(c) \sum_{d=0}^{\infty} \mathcal{T}_d(c) \\
&= S'_1(c) - s - (g - \omega_{\mathcal{T}})S_1(c) + \frac{g}{\mathcal{T}_{\max}} S_1^2(c) \\
&\quad + \frac{g}{\mathcal{T}_{\max}} S_1(c)S_2(c) + \alpha S_3(c)S_1(c) = 0,
\end{aligned} \tag{20}$$

and

$$\begin{aligned}
\sum_{d=1}^{\infty} \Re_d^2(\mathcal{I}_{d-1}(c)) &= \sum_{d=1}^{\infty} \left[\mathcal{I}'_{d-1}(c) - \beta \sum_{p=0}^{d-1} \mathcal{V}_p(c) \mathcal{T}_{d-1-p}(c) + \omega_{\mathcal{I}} \mathcal{I}_{d-1}(c) \right] \\
&= \sum_{d=0}^{\infty} \mathcal{I}'_d(c) - \beta \sum_{d=1}^{\infty} \sum_{p=0}^{d-1} \mathcal{V}_p(c) \mathcal{T}_{d-1-p}(c) + \omega_{\mathcal{I}} \sum_{d=0}^{\infty} \mathcal{I}_d(c) \\
&= \sum_{d=0}^{\infty} \mathcal{I}'_d(c) - \beta \sum_{p=0}^{\infty} \sum_{d=p+1}^{\infty} \mathcal{V}_p(c) \mathcal{T}_{d-1-p}(c) + \omega_{\mathcal{I}} \sum_{d=0}^{\infty} \mathcal{I}_d(c) \\
&= \sum_{d=0}^{\infty} \mathcal{I}'_d(c) - \beta \sum_{p=0}^{\infty} \mathcal{V}_p(c) \sum_{d=0}^{\infty} \mathcal{T}_d(c) + \omega_{\mathcal{I}} \sum_{d=0}^{\infty} \mathcal{I}_d(c) \\
&= S'_2(c) - \beta S_3(c) S_1(c) + \omega_{\mathcal{I}} S_2(c) = 0,
\end{aligned} \tag{21}$$

and finally

$$\begin{aligned}
\sum_{d=1}^{\infty} \Re_d^3(\mathcal{V}_{d-1}(c)) &= \sum_{d=1}^{\infty} \left[\mathcal{V}'_{d-1}(c) - n\omega_b \mathcal{I}_{d-1}(c) + \alpha \sum_{p=0}^{d-1} \mathcal{V}_p(c) \mathcal{T}_{d-1-p}(c) + \omega_{\mathcal{V}} \mathcal{V}_{d-1}(c) \right] \\
&= \sum_{d=0}^{\infty} \mathcal{V}'_d(c) - n\omega_b \sum_{d=0}^{\infty} \mathcal{I}_d(c) + \alpha \sum_{d=1}^{\infty} \sum_{p=0}^{d-1} \mathcal{V}_p(c) \mathcal{T}_{d-1-p}(c) + \omega_{\mathcal{V}} \sum_{d=0}^{\infty} \mathcal{V}_d(c) \\
&= \sum_{d=0}^{\infty} \mathcal{V}'_d(c) - n\omega_b \sum_{d=0}^{\infty} \mathcal{I}_d(c) + \alpha \sum_{p=0}^{\infty} \sum_{d=p+1}^{\infty} \mathcal{V}_p(c) \mathcal{T}_{d-1-p}(c) + \omega_{\mathcal{V}} \sum_{d=0}^{\infty} \mathcal{V}_d(c) \\
&= \sum_{d=0}^{\infty} \mathcal{V}'_d(c) - n\omega_b \sum_{d=0}^{\infty} \mathcal{I}_d(c) + \alpha \sum_{p=0}^{\infty} \mathcal{V}_p(c) \sum_{d=0}^{\infty} \mathcal{T}_d(c) + \omega_{\mathcal{V}} \sum_{d=0}^{\infty} \mathcal{V}_d(c) \\
&= S'_3(c) - n\omega_b S_2(c) + \alpha S_3(c) S_2(c) + \omega_{\mathcal{V}} S_3(c) = 0.
\end{aligned} \tag{22}$$

Eqs. (20), (21) and (22) show that the series solutions $S_1(c)$, $S_2(c)$ and $S_3(c)$ must be the exact solutions of system of equations (1).

4 Numerical investigations

In this section, the HATM is applied to solve the non-linear system of Eqs. (1) for mentioned values of Table 1. Several \hbar -curves are demonstrated in Figs. 1, 2 and 3 for various N to show the regions of convergence. We note that these regions are parallel parts with axiom x . According to these figures, the convergence regions for $N = 5, 10, 15$ are presented in table 2.

Table 2: Regions of convergence for $N = 5, 10, 15$ and $c = 1$.

N	$\hbar_{\mathcal{T}}$	$\hbar_{\mathcal{I}}$	$\hbar_{\mathcal{V}}$
5	$-1.1 \leq \hbar_{\mathcal{T}} \leq -0.9$	$-1.1 \leq \hbar_{\mathcal{I}} \leq -0.8$	$-1.2 \leq \hbar_{\mathcal{V}} \leq -0.7$
10	$-0.8 \leq \hbar_{\mathcal{T}} \leq -0.2$	$-1 \leq \hbar_{\mathcal{I}} \leq -0.2$	$-1 \leq \hbar_{\mathcal{V}} \leq -0.2$
15	$-0.8 \leq \hbar_{\mathcal{T}} \leq -0.2$	$-1 \leq \hbar_{\mathcal{I}} \leq -0.1$	$-1 \leq \hbar_{\mathcal{V}} \leq -0.1$

The approximate solution of problem (1) for $N = 5$ is in the following form

$$\begin{cases} \mathcal{T}_5(c) = 1000 + 5000\hbar + 10000\hbar^2 + \cdots + 0.000017219\hbar^5 c^5, \\ \mathcal{I}_5(c) = -0.0001\hbar c - 0.0006\hbar^2 c + \cdots - 0.0000155458\hbar^5 c^5, \\ \mathcal{V}_5(c) = 0.001 + 0.005\hbar + 0.01\hbar^2 + \cdots + 0.00230941\hbar^5 c^5, \end{cases}$$

and for $N = 10$ we get

$$\begin{cases} \mathcal{T}_{10}(c) = 1000 + 10000\hbar + 45000\hbar^2 + \cdots + 2.00653 \times 10^{-7}\hbar^{10} c^{10}, \\ \mathcal{I}_{10}(c) = -0.0002\hbar c - 0.0027\hbar^2 c + \cdots - 1.81169 \times 10^{-7}\hbar^{10} c^{10}, \\ \mathcal{V}_{10}(c) = 0.001 + 0.01\hbar + 0.045\hbar^2 + \cdots + 0.00002\hbar^{10} c^{10}. \end{cases}$$

Finally, for $N = 15$ the approximate solution is obtained as follows

$$\begin{cases} \mathcal{T}_{15}(c) = 1000 + 15000\hbar + 105000\hbar^2 + \cdots + 1.96276 \times 10^{-10}\hbar^{15} c^{15}, \\ \mathcal{I}_{15}(c) = -0.0003\hbar c - 0.0063\hbar^2 c + \cdots - 1.77216 \times 10^{-10}\hbar^{15} c^{15}, \\ \mathcal{V}_{15}(c) = 0.001 + 0.015\hbar + 0.105\hbar^2 + \cdots + 2.63289 \times 10^{-8}\hbar^{15} c^{15}. \end{cases}$$

Table 3: The residual errors R_1, R_2, R_3 for different values of c and $N = 10$.

c	$R_1(\mathcal{T}_{10}, \mathcal{I}_{10}, \mathcal{V}_{10}; \hbar = -1)$	$R_2(\mathcal{T}_{10}, \mathcal{I}_{10}, \mathcal{V}_{10}; \hbar = -0.8)$	$R_3(\mathcal{T}_{10}, \mathcal{I}_{10}, \mathcal{V}_{10}; \hbar = -0.8)$
0.0	0	1.39264×10^{-9}	7.91347×10^{-9}
0.2	2.67755×10^{-8}	5.67893×10^{-9}	1.51087×10^{-7}
0.4	5.48083×10^{-7}	3.22788×10^{-9}	4.65999×10^{-7}
0.6	3.94648×10^{-6}	1.26519×10^{-8}	5.64987×10^{-7}
0.8	0.0000194632	4.30961×10^{-8}	3.83177×10^{-7}
1.0	0.0000764243	8.41884×10^{-8}	3.73303×10^{-7}

Table 4: The residual errors R_1, R_2, R_3 for different values of c and $N = 15$.

c	$R_1(\mathcal{T}_{15}, \mathcal{I}_{15}, \mathcal{V}_{15}; \hbar = -1)$	$R_2(\mathcal{T}_{15}, \mathcal{I}_{15}, \mathcal{V}_{15}; \hbar = -0.8)$	$R_3(\mathcal{T}_{15}, \mathcal{I}_{15}, \mathcal{V}_{15}; \hbar = -0.8)$
0.0	7.15256×10^{-7}	1.00187×10^{-12}	3.31113×10^{-12}
0.2	4.76837×10^{-7}	1.28466×10^{-11}	2.76486×10^{-10}
0.4	9.53674×10^{-7}	1.24601×10^{-10}	3.15595×10^{-9}
0.6	1.43051×10^{-6}	1.49157×10^{-10}	1.14451×10^{-8}
0.8	3.33786×10^{-6}	2.91038×10^{-10}	1.74332×10^{-8}
1.0	1.90735×10^{-6}	1.52795×10^{-9}	8.58563×10^{-9}

In order to show the efficiency and accuracy of presented method the following residual errors

$$\begin{aligned}
R_1(\mathcal{T}, \mathcal{I}, \mathcal{V}; \hbar) &= \frac{d\mathcal{T}_N(c; \hbar)}{dt} - s + \omega_{\mathcal{T}}\mathcal{T}_N(c; \hbar) \\
&\quad - r\mathcal{T}_N(c; \hbar) \left(1 - \frac{\mathcal{I}_N(c; \hbar) + \mathcal{T}_N(c; \hbar)}{\mathcal{T}_{\max}} \right) \\
&\quad + \alpha\mathcal{V}_N(c; \hbar)\mathcal{T}_N(c; \hbar), \\
R_2(\mathcal{T}, \mathcal{I}, \mathcal{V}; \hbar) &= \frac{d\mathcal{I}_N(c; \hbar)}{dt} - \beta\mathcal{V}_N(c; \hbar)\mathcal{T}_N(c; \hbar) + \omega_{\mathcal{I}}\mathcal{I}_N(c; \hbar), \\
R_3(\mathcal{T}, \mathcal{I}, \mathcal{V}; \hbar) &= \frac{d\mathcal{V}_N(c; \hbar)}{dt} - n\omega_b\mathcal{I}_N(c; \hbar) + \alpha\mathcal{V}_N(c; \hbar)\mathcal{T}_N(c; \hbar) \\
&\quad + \omega_{\mathcal{V}}\mathcal{V}_N(c; \hbar),
\end{aligned} \tag{23}$$

are applied. In Tables 3 and 4 the errors of the residual functions (23) are shown for different values of c and $N = 10, 15$. Also, the errors R_1, R_2, R_3 for various \hbar, c and $N = 5, 10, 15$ are presented in Tables 5, 6 and 7.

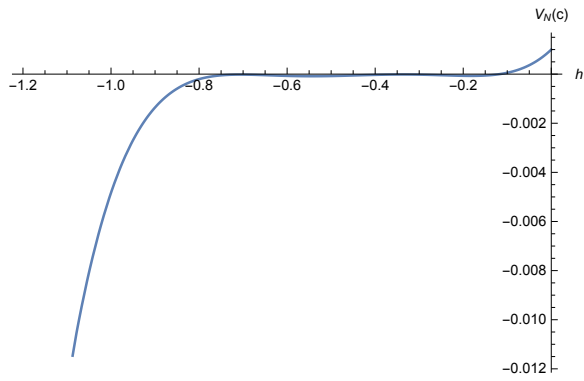
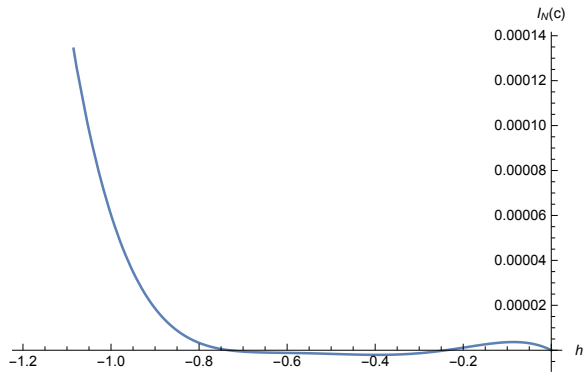
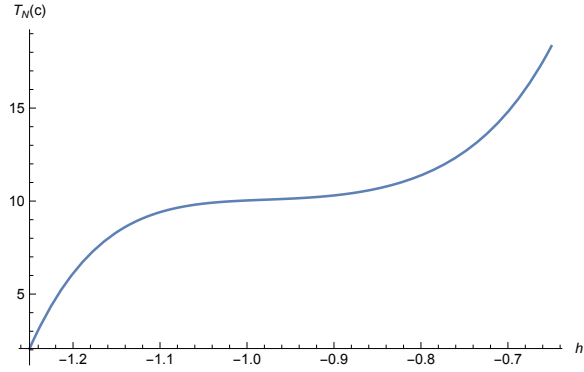


Figure 1: \hbar -curves of $\mathcal{T}_N(c)$, $\mathcal{I}_N(c)$ and $\mathcal{V}_N(c)$ for $N = 5, c = 1$.

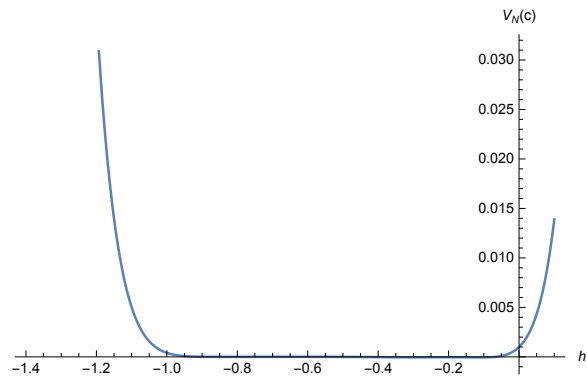
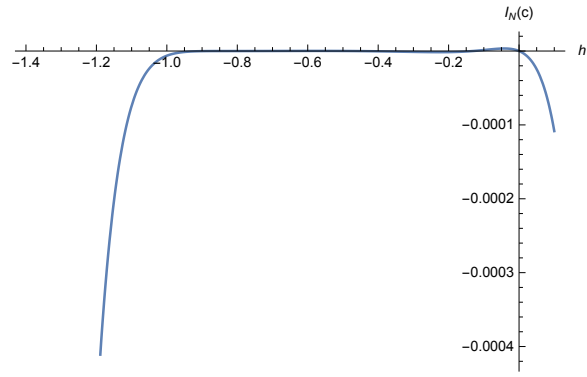
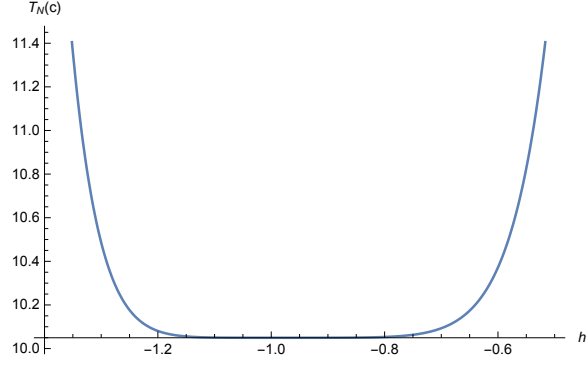


Figure 2: \hbar -curves of $\mathcal{T}_N(c)$, $\mathcal{I}_N(c)$ and $\mathcal{V}_N(c)$ for $N = 10$, $c = 1$.

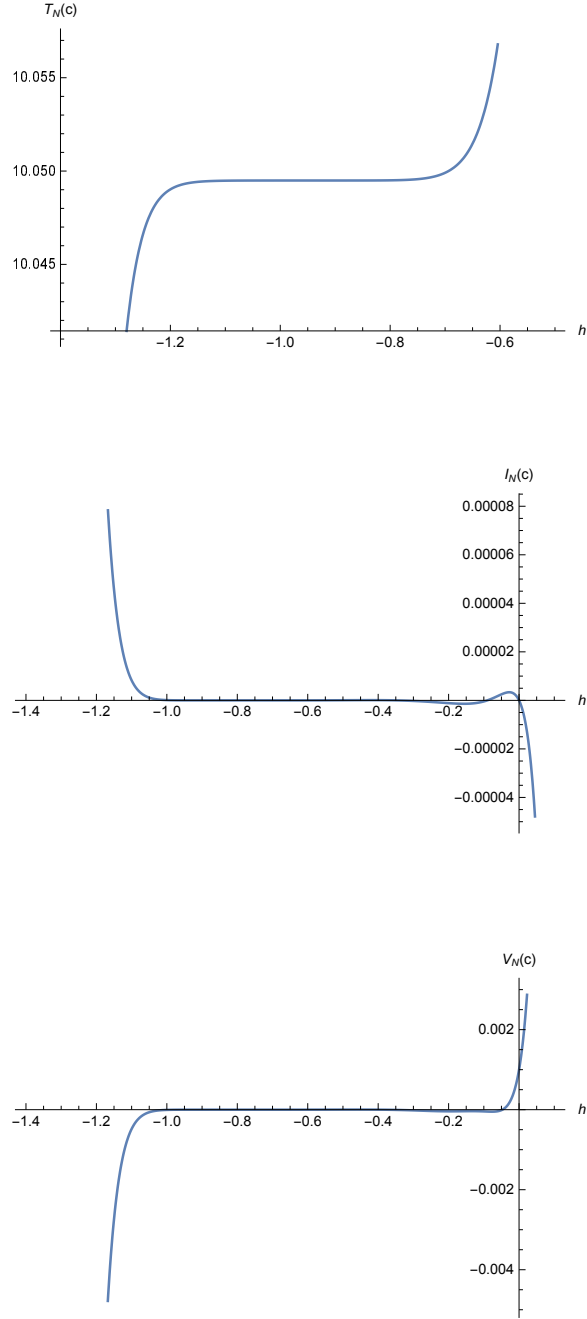


Figure 3: \hbar -curves of $\mathcal{T}_N(c)$, $\mathcal{I}_N(c)$ and $\mathcal{V}_N(c)$ for $N = 15, c = 1$.

Table 5: The numerical results of residual error R_1 for different values of h and $N = 5, 10, 15$.

N	c	$h = -1.2$	$h = -1.1$	$h = -1$	$h = -0.9$	$h = -0.8$	$h = -0.7$
5	0.0	2.3936	0.2473	4.54747×10^{-13}	0.1573	0.953603	2.31402
	0.2	2.86231	0.393719	0.00192233	0.193756	0.97476	2.30218
	0.4	3.3422	0.546942	0.00769465	0.228277	0.995169	2.29027
	0.6	3.83332	0.706994	0.0173277	0.260861	1.01483	2.27832
	0.8	4.33573	0.873909	0.0308357	0.291503	1.03374	2.2663
	1.0	4.84949	1.04772	0.0482368	0.320195	1.0519	2.25423
10	0.0	0.00337716	0.0000109961	0	7.19819×10^{-6}	0.00143155	0.0274381
	0.2	0.00981886	0.000116083	2.67755×10^{-8}	0.0000356712	0.00218667	0.0314455
	0.4	0.019624	0.00036842	5.48083×10^{-7}	0.0000815957	0.00301206	0.0354763
	0.6	0.0335876	0.000853229	3.94648×10^{-6}	0.000146411	0.00390505	0.0395269
	0.8	0.052855	0.00172094	0.0000194632	0.000231558	0.00486306	0.0435937
	1.0	0.0792877	0.00327132	0.0000764243	0.000339417	0.00588353	0.0476735
15	0.0	0.0000190735	5.72205×10^{-6}	7.15256×10^{-7}	0	1.08033×10^{-6}	0.000158743
	0.2	0.0000305176	8.58307×10^{-6}	4.76837×10^{-7}	5.96046×10^{-8}	3.23355×10^{-6}	0.000240277
	0.4	0.0000839233	7.62939×10^{-6}	9.53674×10^{-7}	0	6.4075×10^{-6}	0.000333367
	0.6	0.000236511	7.62939×10^{-6}	1.43051×10^{-6}	8.34465×10^{-7}	0.0000109375	0.000438217
	0.8	0.00088501	0.000038147	3.33786×10^{-6}	0	0.0000168085	0.000554932
	1.0	0.00294495	0.000110626	1.90735×10^{-6}	2.38419×10^{-7}	0.0000242442	0.000683663

Table 6: The numerical results of residual error R_2 for different values of \hbar and $N = 5, 10, 15$.

N	c	$\hbar = -1$	$\hbar = -0.9$	$\hbar = -0.8$	$\hbar = -0.7$	$\hbar = -0.6$	$\hbar = -0.5$	$\hbar = -0.4$	$\hbar = -0.3$	$\hbar = -0.2$
5	0.0	8.67362×10^{-19}	1.53×10^{-7}	8.96002×10^{-7}	2.07912×10^{-6}	3.0741×10^{-6}	3.14453×10^{-6}	1.84893×10^{-6}	4.6405×10^{-7}	1.94852×10^{-6}
	0.2	2.36183×10^{-6}	3.59603×10^{-7}	1.83824×10^{-8}	7.03787×10^{-7}	1.91511×10^{-6}	2.88405×10^{-6}	2.59665×10^{-6}	6.24361×10^{-7}	1.72845×10^{-6}
	0.4	0.0000158382	3.24029×10^{-6}	1.66805×10^{-7}	2.7399×10^{-7}	9.90816×10^{-7}	2.20749×10^{-6}	2.75449×10^{-6}	1.41204×10^{-6}	1.3795×10^{-6}
	0.6	0.0000526939	0.000013953	1.50589×10^{-6}	5.86228×10^{-7}	6.33103×10^{-7}	1.45376×10^{-6}	2.49182×10^{-6}	1.9137×10^{-6}	9.44909×10^{-7}
	0.8	0.000128933	0.0000400706	6.95057×10^{-6}	9.10652×10^{-7}	9.55113×10^{-7}	8.90192×10^{-7}	1.96673×10^{-6}	2.14988×10^{-6}	4.6329×10^{-7}
	1.0	0.000264526	0.000091402	0.0000206229	3.85551×10^{-8}	1.83977×10^{-6}	7.08762×10^{-7}	1.32488×10^{-6}	2.14656×10^{-6}	3.12971×10^{-8}
10	0.0	8.88178×10^{-16}	7.11076×10^{-12}	1.39264×10^{-9}	2.61784×10^{-8}	1.8088×10^{-7}	6.83613×10^{-7}	1.61316×10^{-6}	2.26423×10^{-6}	9.01673×10^{-7}
	0.2	1.16239×10^{-9}	2.9645×10^{-10}	5.67893×10^{-9}	3.01391×10^{-8}	3.37891×10^{-8}	1.58873×10^{-7}	8.46232×10^{-7}	1.87794×10^{-6}	1.5073×10^{-6}
	0.4	9.90321×10^{-8}	3.27009×10^{-9}	3.22788×10^{-9}	6.49721×10^{-8}	1.43943×10^{-7}	7.98264×10^{-8}	3.8955×10^{-7}	1.43543×10^{-6}	1.77257×10^{-6}
	0.6	1.49498×10^{-6}	1.84515×10^{-8}	1.26519×10^{-8}	8.15485×10^{-8}	2.30731×10^{-7}	1.98717×10^{-7}	1.77066×10^{-7}	1.06296×10^{-6}	1.8029×10^{-6}
	0.8	0.0000108751	2.1865×10^{-7}	4.30961×10^{-8}	8.28309×10^{-8}	3.10485×10^{-7}	2.9468×10^{-7}	1.19973×10^{-7}	8.20621×10^{-7}	1.68352×10^{-6}
	1.0	0.0000525467	1.77104×10^{-6}	8.41884×10^{-8}	7.48912×10^{-8}	3.8044×10^{-7}	4.06603×10^{-7}	1.34283×10^{-7}	7.22977×10^{-7}	1.48205×10^{-6}
15	0.0	1.59162×10^{-12}	1.13687×10^{-13}	1.00187×10^{-12}	1.54×10^{-10}	4.59024×10^{-9}	5.49317×10^{-8}	3.44807×10^{-7}	1.22125×10^{-6}	2.00388×10^{-6}
	0.2	1.45519×10^{-11}	3.63798×10^{-12}	1.28466×10^{-11}	4.77598×10^{-10}	6.29957×10^{-9}	1.96057×10^{-8}	5.14657×10^{-8}	6.0141×10^{-7}	1.74667×10^{-6}
	0.4	8.73115×10^{-11}	1.45519×10^{-11}	1.24601×10^{-10}	4.50314×10^{-10}	1.02114×10^{-8}	5.85214×10^{-8}	8.89341×10^{-8}	2.45201×10^{-7}	1.41322×10^{-6}
	0.6	5.41331×10^{-9}	4.36557×10^{-11}	1.49157×10^{-10}	3.06818×10^{-9}	6.67617×10^{-9}	8.18413×10^{-8}	1.69766×10^{-7}	6.71273×10^{-8}	1.10776×10^{-6}
	0.8	1.16648×10^{-7}	1.16415×10^{-10}	2.91038×10^{-10}	6.66932×10^{-9}	3.37855×10^{-9}	9.46372×10^{-8}	2.34552×10^{-7}	9.33337×10^{-9}	8.82618×10^{-7}
	1.0	1.27265×10^{-6}	1.39698×10^{-9}	1.52795×10^{-9}	1.04319×10^{-8}	1.89696×10^{-8}	9.87109×10^{-8}	2.98313×10^{-7}	4.19607×10^{-8}	7.55504×10^{-7}

Table 7: The numerical results of residual error R_3 for different values of h and $N = 5, 10, 15$.

N	c	$h = -1$	$h = -0.9$	$h = -0.8$	$h = -0.7$	$h = -0.6$	$h = -0.5$	$h = -0.4$	$h = -0.3$	$h = -0.2$	$h = -0.1$
5	0.0	8.67362×10^{-18}	8.724×10^{-7}	0.0000135168	0.0000597131	0.000156055	0.000296227	0.000433237	0.000461549	0.000198946	0.000632101
	0.2	0.000129472	3.88679×10^{-6}	0.0000232311	0.0000367519	0.0000380235	0.0000855291	0.000223225	0.000400997	0.000394736	0.000274581
	0.4	0.00135862	0.000177259	7.51081×10^{-6}	0.0000564347	0.0000381277	0.0000198935	0.0000296976	0.000260365	0.000477599	0.0000232641
	0.6	0.00583374	0.00124183	0.0000647749	0.0000352512	0.0000876229	0.0000240495	0.000107956	0.0000835355	0.000471531	0.000266178
	0.8	0.017109	0.0046054	0.000574488	0.0000322082	0.000113154	0.0000442726	0.00016974	0.0000946753	0.000398158	0.000458718
	1.0	0.0404312	0.0125307	0.00229039	0.0000254373	0.0000588742	0.000140393	0.000152141	0.000247825	0.000276823	0.00060526
10	0.0	8.88178×10^{-16}	1.28284×10^{-11}	7.91347×10^{-9}	2.85089×10^{-7}	3.30616×10^{-6}	0.0000202734	0.0000802982	0.000220035	0.000385465	0.0000947121
	0.2	4.92029×10^{-8}	4.72683×10^{-9}	1.51087×10^{-7}	2.10356×10^{-8}	3.15451×10^{-6}	0.000011795	0.0000284061	0.0000862038	0.000263189	0.000290276
	0.4	5.84654×10^{-6}	6.25106×10^{-8}	4.65999×10^{-7}	1.54108×10^{-6}	4.21028×10^{-7}	0.0000109938	0.0000191687	0.0000153365	0.000131322	0.000390522
	0.6	0.000109276	1.85419×10^{-7}	5.64987×10^{-7}	3.14461×10^{-6}	2.74231×10^{-6}	8.67918×10^{-6}	0.0000254225	6.65097×10^{-6}	0.0000152451	0.000417307
	0.8	0.00093273	0.0000128647	3.83177×10^{-7}	4.83092×10^{-6}	5.14217×10^{-6}	4.8722×10^{-6}	0.0000315151	2.60466×10^{-6}	0.0000712265	0.000389391
	1.0	0.00512464	0.000139456	3.73303×10^{-7}	6.37062×10^{-6}	7.49196×10^{-6}	2.3893×10^{-6}	0.0000314601	0.000026181	0.00012284	0.000322735
15	0.0	2.27374×10^{-13}	2.27374×10^{-13}	3.31113×10^{-12}	9.86057×10^{-10}	4.98968×10^{-8}	9.59473×10^{-7}	9.74223×10^{-6}	0.0000603884	0.000229812	0.000330239
	0.2	0	2.72848×10^{-12}	2.76486×10^{-10}	1.5668×10^{-8}	4.30215×10^{-8}	7.57963×10^{-7}	5.88135×10^{-6}	0.0000229083	0.000103157	0.000342435
	0.4	3.8126×10^{-9}	1.09139×10^{-10}	3.15595×10^{-9}	3.00904×10^{-8}	3.66815×10^{-7}	5.20925×10^{-7}	4.20601×10^{-6}	0.0000143819	0.0000268466	0.000289918
	0.6	3.14903×10^{-7}	1.01863×10^{-9}	1.14451×10^{-8}	1.30044×10^{-8}	5.98062×10^{-7}	1.85369×10^{-6}	2.01119×10^{-6}	0.0000163409	7.71528×10^{-6}	0.000201946
	0.8	7.62218×10^{-6}	2.2701×10^{-9}	1.74332×10^{-8}	1.26489×10^{-7}	6.84324×10^{-7}	2.97462×10^{-6}	4.24188×10^{-7}	0.0000192142	0.0000125839	0.000100126
	1.0	0.0000949907	5.54137×10^{-8}	8.58563×10^{-9}	3.07671×10^{-7}	6.09615×10^{-7}	3.99947×10^{-6}	2.38387×10^{-6}	0.000019579	5.39521×10^{-9}	2.04689×10^{-7}

5 Conclusion

The mathematical model of HIV infection for $CD4^+T$ cells is an applicable and robust model to analyze, track and control the infection. In this study, the HATM was introduced by combining the Laplace transformations and the HAM to approximate the presented model. The obtained solution of HATM depends on auxiliary parameters and functions specially the convergence control parameter \hbar . It is useful tool to identify and control the region of convergence. Existence of auxiliary functions and parameters are the advantages of the HATM which transformed the presented method to the flexible and applicable scheme than the other semi-analytical methods. Furthermore, the convergence theorem was proved to support the HATM analytically. The rate of convergence depends on parameter \hbar . In order to show the regions of convergence some \hbar -curves were plotted for $N = 5, 10, 15$. The efficiency and accuracy of method were shown by applying the errors of residual functions. The numerical errors based on the residual functions were obtained for different values of convergence control parameter \hbar and number of iteration N .

References

- [1] S. Abbasbandy, Homotopy analysis method for heat radiation equations, *International Communications in Heat and Mass Transfer*, 34, 380-387 (2007).
- [2] S. Abbasbandy, E. Shivanian, K. Vajravelu, Mathematical properties of \hbar -curve in the frame work of the homotopy analysis method, *Commun Nonlinear Sci Numer Simulat*, 16, 4268-4275 (2011).
- [3] S. Abbasbandy, M. Jalili, Determination of optimal convergence-control parameter value in homotopy analysis method, *Numer Algor*, 64(4), 593-605 (2013).
- [4] M. Ahmadi, H. Sartipizadeh, E. Ozkan, A new pressure-rate deconvolution algorithm based on Laplace transformation and its application to measured well responses, *Journal of Petroleum Science and Engineering*, 157, 68-80 (2017).
- [5] F. Chen, Q.Q. Liu, Adomian decomposition method combined with Padé approximation and Laplace transform for solving a model of HIV infection of $CD4^+T$ cells, *Discrete Dynamics in Nature and Society*, (2015).
- [6] R.V. Culshaw, S. Ruan, A delay-differential equation model of HIV infection of $CD4^+T$ -cells, *Mathematical Biosciences*, 165, 27-39 (2000).
- [7] N. Dogan, Numerical treatment of the model for HIV infection of $CD4^+T$ cells by using multistep Laplace-Adomian decomposition method, *Discrete Dynamics in Nature and Society*, 2012, (2012).
- [8] G.I. El-Baghdady, M.M. Abbas, M.S. El-Azab, R.M. El-Ashwah, The spectral collocation method for solving (HIV-1) via Legendre polynomials, *Int. J. Appl. Comput. Math.*, (2017).

- [9] M.A. Fariborzi Araghi, Sh. Behzadi, Numerical solution of nonlinear Volterra-Fredholm integro-differential equations using homotopy analysis method, *Journal of Applied Mathematics and Computing*, 37, (2011).
- [10] M.A. Fariborzi Araghi, A. Fallahzadeh, On the convergence of the homotopy analysis method for solving the Schrodinger equation, *Journal of Basic and Applied Scientific Research*, 2(6), 6076-6083 (2012).
- [11] M.A. Fariborzi Araghi, A. Fallahzadeh, Explicit series solution of Boussinesq equation by homotopy analysis method, *Journal of American Science*, 8 (11), (2012).
- [12] M.A. Fariborzi Araghi, S. Noeiaghdam, A novel technique based on the homotopy analysis method to solve the first kind Cauchy integral equations arising in the theory of airfoils, *Journal of Interpolation and Approximation in Scientific Computing*, 2016 (1), 1-13 (2016).
- [13] M.A. Fariborzi Araghi, S. Noeiaghdam, Homotopy analysis transform method for solving generalized Abel's fuzzy integral equations of the first kind, *IEEE*, (2016).
- [14] M.A. Fariborzi Araghi, S. Noeiaghdam, Homotopy regularization method to solve the singular Volterra integral equations of the first kind, *Jordan Journal of Mathematics and Statistics*, 10(4), (2017).
- [15] A.A. Freihat, M. Zurigat, A. H. Handam, The multi-step homotopy analysis method for modified epidemiological model for computer viruses, *Afrika Matematika*, 26, 585-596 (2015).
- [16] A. Gökdoğan, A. Yildirim, M. Merdan, Solving a Fractional order model of HIV infection of $CD4^+$ T cells, *Math. Comput. Model.*, 54(9), 2132-2138 (2011).
- [17] M. Ghoreishi, A.M. Ismail, A. Alomari, Application of the Homotopy analysis method for solving a model for HIV infection of $CD4^+$ T-cells, *Math. Comput. Model.*, 54(11), 3007-3015 (2011).
- [18] F. Guerrero, F.J. Santonja, R.J. Villanueva, Solving a model for the evolution of smoking habit in Spain with homotopy analysis method, *Nonlinear Analysis: Real World Applications*, 14, 549-558 (2013).
- [19] X. Han, Q. Tan, Dynamical behavior of computer virus on Internet, *Appl. Math. Comput.*, 217, 2520-2526 (2010).
- [20] M. Khan, M. Asif Gondal, I. Hussain, S. Karimi Vanani, A new comparative study between homotopy analysis transform method and homotopy perturbation transform method on a semi infinite domain, *Mathematical and Computer Modelling*, 55(3-4), 1143-1150 (2012).
- [21] Y. Khan, H. Vazquez-Leal, N. Faraz, An auxiliary parameter method using Adomian polynomials and Laplace transformation for nonlinear differential equations, *Applied Mathematical Modelling*, 37(5), 2702-2708 (2013).

- [22] E. Khoshrouye Ghiasi, R. Saleh, Homotopy analysis method for the Sakiadis flow of a thixotropic fluid, *Eur. Phys. J. Plus*, 134(1), (2019), 1-9. <https://doi.org/10.1140/epjp/i2019-12449-9>
- [23] E. Khoshrouye Ghiasi, R. Saleh, Nonlinear stability and thermomechanical analysis of hydromagnetic Falkner-Skan Casson conjugate fluid flow over an angular-geometric surface based on Buongiorno's model using homotopy analysis method and its extension, *Pramana*, 92(1), (2019), 1-12. <https://doi.org/10.1007/s12043-018-1667-1>
- [24] E. Khoshrouye Ghiasi, R. Saleh, 2D flow of Casson fluid with non-uniform heat source/sink and Joule heating, *Front. Heat Mass Trans.*, 12, (2019), 1-7. <https://doi.org/10.5098/hmt.12.4>
- [25] E. Khoshrouye Ghiasi, R. Saleh, Analytical and numerical solutions to the 2D Sakiadis flow of Casson fluid with cross diffusion, inclined magnetic force, viscous dissipation and thermal radiation based on Buongiorno's mathematical model, *CFD Lett.*, 11(1), (2019), 40-54.
- [26] E. Khoshrouye Ghiasi, R. Saleh, Unsteady shrinking embedded horizontal sheet subjected to inclined Lorentz force and Joule heating, an analytical solution, *Results Phys.*, 11, (2018), 65-71. <https://doi.org/10.1016/j.rinp.2018.07.026>
- [27] E. Khoshrouye Ghiasi, R. Saleh, Constructing analytic solutions on the Tricomi equation, *Open Phys.*, 16(1), (2018), 143-148. <https://doi.org/10.1515/phys-2018-0022>
- [28] E. Khoshrouye Ghiasi, R. Saleh, Non-dimensional optimization of magnetohydrodynamic Falkner-Skan fluid flow, *INAE Lett.*, 3(3), (2018), 143-147. <https://doi.org/10.1007/s41403-018-0043-2>
- [29] M. Komeili, C. Menon, Modelling the dynamic response of a micro-cantilever excited at its base by an arbitrary thermal input using Laplace transformation, *Applied Mathematical Modelling*, 43, 481-497 (2017).
- [30] W. Kong, B. Perers, J. Fan, S. Furbo, F. Bava, A new Laplace transformation method for dynamic testing of solar collectors, *Renewable Energy*, 75, 448-458 (2015).
- [31] S. Kumar, J. Singh, D. Kumar, S. Kapoor, New homotopy analysis transform algorithm to solve volterra integral equation, *Ain Shams Eng J.*, 5, 243-246 (2014).
- [32] D. Kumar, J. Singh, Sushila, Application of homotopy analysis transform method to fractional biological population model, *Romanian Reports in Physics*, 65, 63-75 (2013).
- [33] S. Kumar, D. Kumar, Fractional modelling for BBM-Burger equation by using new homotopy analysis transform method, *Journal of the Association of Arab Universities for Basic and Applied Sciences*, 16, 16-20 (2014).
- [34] D. Kumar, J. Singh, S. Kumar, Sushila, Numerical computation of Klein-Gordon equations arising in quantum field theory by using homotopy analysis transform method, *Alexandria Engineering Journal*, 53(2), 469-474 (2014).

- [35] S.J. Liao, The proposed homotopy analysis techniques for the solution of nonlinear problems, Ph.D. Thesis, Shanghai Jiao Tong University, Shanghai, (1992) (in English).
- [36] S.J. Liao, Beyond Perturbation: Introduction to Homotopy Analysis Method, Chapman & Hall/CRC Press, Boca Raton, (2003).
- [37] S.J. Liao, On the homotopy analysis method for nonlinear problems, Appl. Math. Comput., 147, 499-513 (2004).
- [38] S.J. Liao, Homotopy analysis method in nonlinear differential equations, Higher Education Press, Beijing and Springer-Verlag Berlin Heidelberg, (2012).
- [39] S.J. Liao, Y. Tan, A general approach to obtain series solutions of nonlinear differential equations, Stud. Appl. Math., 119, 297-355 (2007).
- [40] M. Merdan, A. Gökdoğan, A. Yildirim, On the numerical solution of the model for HIV infection of $CD4^+$ T cells, Comput. Math. Appl., 62(1), 118-123 (2011).
- [41] S. Noeiaghdam, A novel technique to solve the modified epidemiological model of computer viruses, SeMA Journal, (2018). <https://doi.org/10.1007/s40324-018-0163-3>.
- [42] S. Noeiaghdam, M.A. Fariborzi Araghi, S. Abbasbandy, Finding optimal convergence control parameter in the homotopy analysis method to solve integral equations based on the stochastic arithmetic, Numer Algor (2018). <https://doi.org/10.1007/s11075-018-0546-7>.
- [43] S. Noeiaghdam, M. Suleman, H. Budak, Solving a modified nonlinear epidemiological model of computer viruses by homotopy analysis method, Mathematical Sciences, 1-12 (2018). <https://doi.org/10.1007/s40096-018-0261-5>
- [44] S. Noeiaghdam, E. Zarei, H. Barzegar Kelishami, Homotopy analysis transform method for solving Abel's integral equations of the first kind, Ain Shams Eng. J., 7, 483-495 (2016).
- [45] M.Y. Ongun, The Laplace Adomian decomposition method for solving a model for HIV infection of $CD4^+$ T cells, Math. Comput. Model., 53(5), 597-603 (2011).
- [46] N. Ozalp, O. Ozturk Mizrak, Fractional Laplace transform method in the framework of the CTIT transformation, Journal of Computational and Applied Mathematics, 317, 90-99 (2017).
- [47] Y. Oztürk, M. Gülsu, Numerical solution of a modified epidemiological model for computer viruses, Applied Mathematical Modelling, 39, 7600-7610 (2015).
- [48] K. Parand, S. Latifi, M. M. Moayeri, Shifted Lagrangian Jacobi collocation scheme for numerical solution of a model of HIV infection, SeMA Journal, 1-20 (2017).
- [49] A.S. Perelson, Modelling the interaction of the immune system with HIV, in: C. Castillo-Chavez (Ed.), Mathematical and Statistical Approaches to AIDS Epidemiology, Springer, Berlin, p. 350 (1989).

- [50] A.S. Perelson, D.E. Kirschner, R. De Boer, Dynamics of HIV infection of CD4⁺ T-cells, *Mathematical Biosciences*, 114, (1993).
- [51] B. Prakash, A. Setia, D. Alapatt, Numerical solution of nonlinear fractional SEIR epidemic model by using Haar wavelets, *Journal of Computational Science*, 22, 109-118 (2017).
- [52] W. Sikander, U. Khan, N. Ahmed, S.T. Mohyud-Din, Optimal solutions for a bio mathematical model for the evolution of smoking habit, *Results in Physics*, 7, 510-517 (2017).
- [53] V.K. Srivastava, M.K. Awasthi, S. Kumar, Numerical approximation for HIV infection of CD4⁺T cells mathematical model, *Ain Shams Eng. J.*, 5(2), 625-629 (2014).
- [54] H. Vazquez-Leal, F. Guerrero, Application of series method with Pad and Laplace-Padé resummation methods to solve a model for the evolution of smoking habit in Spain, *Computational and Applied Mathematics*, 33 (1), 181-192 (2014).
- [55] S. Venkatesh, S.R. Balachandar, S. Ayyaswamy, K. Balasubramanian, A new approach for solving a model for HIV infection of CD4⁺T cells arising in mathematical chemistry using Wavelets, *J. Math. Chem.*, 54(5), 1072-1082 (2016).
- [56] L. Yakob, Endectocide-treated cattle for malaria control: A coupled entomological-epidemiological model, *Parasite Epidemiology and Control*, 1, 2-9 (2016).
- [57] Ş. Yüzbaşı, A numerical approach to solve the model for HIV infection of CD4⁺T cells, *Appl. Math. Model.*, 36(12), 5876-5890 (2012).
- [58] Ş. Yüzbaşı, M. Karaçayır, An exponential Galerkin method for solutions of HIV infection model of CD4⁺T-cells, *Computational Biology and Chemistry*, 67, 205-212 (2017).
- [59] M. Zurigat, M. Ababneh, Application of the multi-step differential transform method to solve a Fractional human T-cell Lymphotropic virus I (HTLV-I) infection of CD4⁺T cells, *J. Math. Appl.*, 38, 171-180 (2015).